Journal of Marine Research, 60, 255–279, 2002

Mixing in the surface waters of the western Bay of Bengal using ^{228}Ra and ^{226}Ra

by R. Rengarajan[1], M. M. Sarin[1], B. L. K. Somayajulu[1,2] and R. Suhasini[1,3]

ABSTRACT

^{228}Ra and ^{226}Ra have been measured in the surface waters of the western Bay of Bengal during five cruises conducted between 1988 and 1999. The ranges and mean (given in brackets) concentrations for ^{228}Ra and ^{226}Ra are 6.8–42.1 (17.8 ± 7.9) dpm/100 kg and 6.0–16.7 (9.2 ± 2.2) dpm/100 kg, respectively. (^{228}Ra/^{226}Ra) Activity Ratio (henceforth denoted as [228/226]) ranges from 0.8 to 3.4 with a mean of 1.9 ± 0.5. Both ^{228}Ra and ^{226}Ra show inverse correlation with salinity, the former much stronger.

A surface 2-D diffusion-advection model is used with a new approach. A simple bivariate function,

$$C_{(x,y)} = C_0 e^{-Ax} \cdot e^{-By}$$

where C_0, A and B are constants, is fitted to the whole ^{228}Ra and ^{226}Ra data $C_{(x,y)}$. Substituting $C_{(x,y)}$ in the two-dimensional steady-state diffusion equation of Ra, the estimated values of the constants A and B can be related to eddy diffusivities and advection velocities in the zonal (x) and meridional (y) directions. From this relationship, the horizontal eddy diffusivities in the zonal and meridional directions are inferred to be 1.3×10^7 and 2.1×10^8 cm^2 s^{-1}, respectively in the absence of advection terms. Similarly, neglecting the influence of diffusion, one can estimate the advection velocities, w_x and w_y in the zonal and meridional directions, as 0.2 and 1.1 cm s^{-1}, respectively. The model-fit values $C_{(x,y)}$ of ^{228}Ra concentrations are in good agreement with the measured values except in regions showing exceptionally high and low values. Incorporating both the advection rates and eddy diffusivities into the equation, it is found that increasing advection velocities depending on the direction can decrease or increase the eddy diffusivities and that such changes are more effective in the meridional direction compared to zonal direction in the region of study.

On the whole, ^{228}Ra appears a good tracer to derive rates of mixing between low salinity waters in the north and their high salinity southern counterparts of the western Bay of Bengal. The eddy diffusivities, K_x and K_y (without advection) derived for the Bay of Bengal are higher by about an order of magnitude than the ones similarly obtained for the Arabian Sea. This is not unexpected due to the turbulent conditions prevailing in the Bay of Bengal for most of the year.

1. Physical Research Laboratory, Ahmedabad 380 009, India.
2. Corresponding author: ***email: soma@prl.ernet.in***
3. Present address: G3, Shirdi Apartments, Somajiguda, Hyderabad 500 082, India.

1. Introduction

Radium isotopes have long been useful in studying the mixing of water in the ocean (Koczy, 1958). The evaluation of both small-scale and large-scale mixing across and within ocean basins is possible from the determination of naturally occurring Ra isotopes, ^{224}Ra ($t_{1/2}$ = 3.64 d), ^{223}Ra (=11.4 d), ^{228}Ra (=5.75 y) and ^{226}Ra (=1600 y) (Sarmiento *et al.,* 1982; Torgersen *et al.,* 1996; Moore, 1999). Ra isotopes enter the ocean mainly through riverine and stream discharges or at the sediment-water boundary—be it the continental margin or deep ocean region. Ra diffuses into water from sediment and this release is maximal in estuarine regions (salinity ~2–20 —Elsinger and Moore, 1983). The half-life of ^{228}Ra is well suited for studying oceanic processes occurring on ~1 to ~30 y time scales (Broecker *et al.,* 1976; Chung, 1980; Ku and Luo, 1994; Schmidt and Reyss, 1996). Utilizing a simple and elegant extraction technique (Moore, 1976), it is possible to routinely measure ^{226}Ra and ^{228}Ra in horizontal and vertical profiles to derive circulation parameters like eddy diffusivities, both lateral and vertical in the surface and deep layers of the ocean (Nozaki *et al.,* 1990; Rutgers Van der Loeff *et al.,* 1995; Somayajulu *et al.,* 1996; Huh and Ku, 1998). The geochemistry of the Ra isotopes is well established, as demonstrated during the GEOSECS expeditions to the world oceans in the seventies (Broecker *et al.,* 1976; Chung, 1980).

Oceanographically, the Bay of Bengal is a very important region wherein seven large rivers (six from India and Irrawaddy River from Myanmar) annually discharge ~10^{15} g sediment and ~10^{15} liters of water, a major fraction of which is contributed by the Ganga-Brahmaputra River estuarine system itself (UNESCO, 1971; Milliman, 1981; Milliman and Meade, 1983). Carroll *et al.* (1993) estimated that 9.5×10^{14} dpm y^{-1} is the ^{226}Ra input to the Bay from the Ganga-Brahmaputra River estuarine (known as the Meghna River in Bangladesh) system alone. From the available data on ^{228}Ra and ^{226}Ra in the Meghna (Carroll, 1990) and in the Hooghly (Somayajulu *et al.,* 2002) estuaries, it is estimated that (1–3) $\times$ 10^{15} dpm y^{-1} of ^{228}Ra is added to the Bay of Bengal from the Ganga-Brahmaputra River system itself. With such a large input of Ra isotope, it should be possible to study mixing in both the surface and subsurface waters of the Bay of Bengal (Sarin *et al.,* 1994). As part of the program initiated in the laboratory to study mixing in the northern Indian Ocean using ^{14}C and Ra isotopes, the surface to 500 m of the water column is being sampled for Ra isotopes. In this paper we report the Ra isotope (^{228}Ra and ^{226}Ra) measurements in the surface waters of the western Bay of Bengal collected during five cruises in an attempt to understand its distribution and to derive 1-D and 2-D model-based lateral eddy diffusivities and advection velocities in the zonal and meridional directions in the region using ^{228}Ra.

2. Materials and methods

Radium isotope measurements were made on 72 surface seawater samples collected in the western Bay of Bengal (Figs. 1a, b and c) during five different cruises. These are G-200 (August–September 1988) on board R/V *Gaveshani,* SK-63 (March–April 1991), SK-70

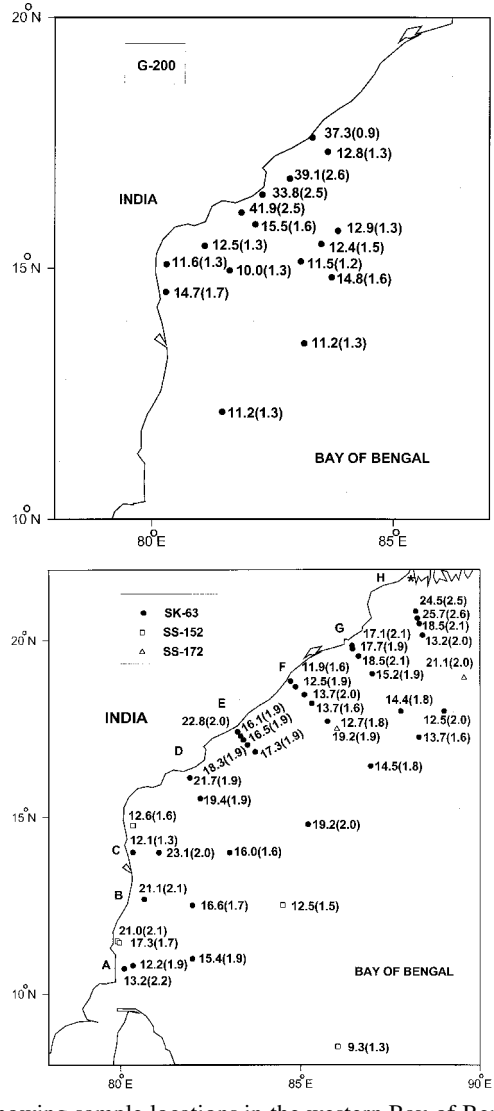

Figure 1(a–c). Maps showing sample locations in the western Bay of Bengal. The numbers given adjacent to the locations are ^{228}Ra concentration (dpm/100 kg) and [228/226] in brackets. Details are given in Table 1. (a) Samples collected during Aug.–Sep. 1988 onboard R/V *Gaveshani*. (b) Samples collected on board ORV *Sagar Kanya* (March–April 1991) and FORV *Sagar Sampada* (February 1997, 1999). Two of the SS-172 samples fall slightly outside the figure but are used for model calculations. The asterisk (*) denotes the origin from where the distances in both *x* and *y* directions are computed for model calculations. (c) Samples collected on board ORV *Sagar Kanya* during December 1991. Coast-to-open-ocean tracks A to H of SK-63 and SK-70 cruises are indicated along the coast (b and c).

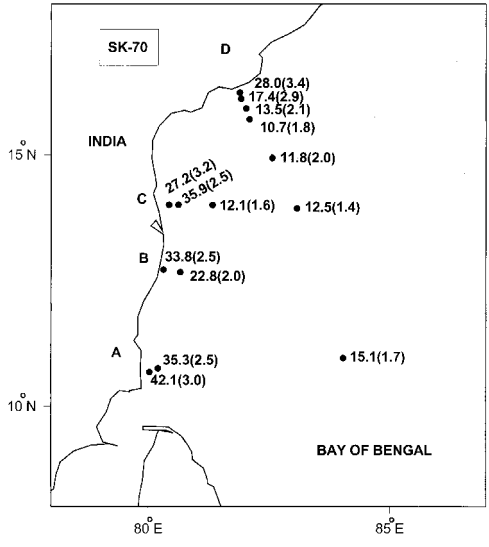

Figure 1(a–c). (Continued)

(December 1991) both on board ORV *Sagar Kanya* and SS-152 (February 1997), SS-172 (February 1999) both on board FORV *Sagar Sampada.* The SK-63 cruise covered most of the EEZ of the Bay of Bengal coast of India (Fig. 1b) whereas the SK-70 cruise taken during December 1991 covered the southern part of the area (Fig. 1c). During the SS-152 and SS-172 cruises only 5 and 4 samples, respectively, falling in the study area (Fig. 1b) are used. During all these cruises, 100 L surface water samples were collected using either 100 L GoFlo bottles or four 30 L GoFlo bottles fixed on a rosette and these samples were transferred into clean plastic drums. Seawater was passed at the rate of ~2 to 3 L h^{-1} through two Plexiglas columns in series (2 cm diameter × 20 cm length) which were packed with MnO_2 fiber (Moore, 1976). Salinity and water temperature were recorded at the stations and the fiber samples were brought to the laboratory. The Ra isotopes, along with Mn from the fiber samples, were brought into solution by boiling with 2M HCl and were co-precipitated with $BaSO_4$ after Ba carrier addition and homogenization. The $BaSO_4$ amounting to 500 mg was dried, weighed and sealed in a plastic vial and was assayed for Ra isotopes after three weeks from sealing the vial to allow ^{222}Rn and its daughters to grow into equilibrium with ^{226}Ra. Samples were counted in a Canberra Model GCW 2523 coaxial well type, intrinsic HPGe detector with a well depth of 35 mm and diameter of 20.5 mm which was calibrated (Moore, 1984; Somayajulu *et al.,* 1999). Standards were made from $BaSO_4$ doped with U (4 and 2%) and monazite NBS standards as well as calibrated ^{226}Ra standard. They were counted periodically to check the constancy of the efficiencies of the gamma detector during the counting period. The detector is shielded with 15-cm thick lead to reduce the background activity. $BaSO_4$ blanks (500 mg recovered using the same procedure without passing seawater) were also counted periodically. The

resolution of the detector is 1.4 keV (FWHM) at 1.22 MeV. Precision of this analytical technique is ±5% (1σ) based on multiple analyses of several standards used for calibration. Whenever there was a delay between sample collection and counting (by more than one month), the ^{228}Ra data were decay-corrected to the date of collection. Since the time delay was less than ~2 years in extreme cases, no corrections were necessary for ^{226}Ra. Generally, it took 3–4 days counting time to achieve a statistical uncertainty of ~10% on the final Ra isotope concentrations (Table 1).

3. Hydrography of the western Bay of Bengal

Many workers (La Fond and La Fond, 1968; Wyrtki, 1971; Potemra *et al.,* 1991; Vinaychandran, 1995; Shetye *et al.,* 1996) have described the physical oceanography of the Bay of Bengal. The monsoon winds that sweep across the north Indian Ocean force considerable seasonal changes in surface circulation. The East India Coastal Current (EICC) is best developed in March–April, when winds in the region of the current are the weakest during the year. Though winds over the north Indian Ocean are much stronger during the southwest monsoon (June–September), the circulation along the coast of India is better organized during the northeast monsoon (November–January). The current carries low-salinity waters that originate in the northern Bay due to river runoff, especially from the Ganga-Brahmaputra rivers. The EICC transports these waters all the way to the southwest coast of India after turning around Sri Lanka. From there the western India Coastal Current (WICC) carries them northward along the west coast of India (Shetye, 1999).

The mixed layer depth (D_{ml}) in the western Bay of Bengal varies from ~40 m to ~80 m but averages around 50 m for the most part of the year (Wyrtki, 1971; Shetye, 1993; Varkey *et al.,* 1996). It is shallower toward the coast than farther offshore. Average values of temperature and salinity observed in the region are 27°C and 32, respectively (Shetye *et al.,* 1996). The mean annual-surface-salinity distribution in the Bay of Bengal in general is unique. The north, northwestern and northeastern regions are noted for maximum freshwater discharge which results in low salinity waters (31) which increases to ~34 south toward equator (Fig. 2). Overall, the surface salinity pattern does not significantly change during different seasons (Wyrtki, 1971; Levitus, 2001).

Abnormal increases in the elevation of the sea surface above its mean level have led to well-documented cases of flooding with consequential loss of life and property in the low-lying areas adjacent to the Bay of Bengal. These increases can be produced by a combination of effects of the astronomical tides, wind-generated surges forced by tropical cyclones and freshwater outflow from the river systems (Johns, 1981). While returning to the Bay such tidal waters can bring in Ra isotopes leached from the soil and suspended sediments but these are not perennial like river discharges. The Bay of Bengal is well known as a source of cyclonic storms for about 75% of the year. These storms generally move into Bangladesh and the east coast of India (Pant and Rupa Kumar, 1997). All these

Table 1. Concentrations of Ra isotopes, temperature and salinity.

Station	Location	Temp °C	Salinity	^{228}Ra* (dpm/100 kg)	^{226}Ra* (dpm/100 kg)	[228/226]*
G-200 (August–September 1988)						
4884	15°44.7′N 83°51.6′E	29.4	33.01	12.9 ± 1.2	9.9 ± 0.8	1.3 ± 0.1
4886	16°47.0′N 82°51.7′E	29.7	29.36	39.1 ± 3.5	14.9 ± 0.6	2.6 ± 0.2
4890	16°27.8′N 82°17.6′E	28.7	33.60	33.8 ± 2.0	13.8 ± 0.7	2.5 ± 0.1
4892	16°6.5′N 81°51.5′E	28.8	31.90	41.9 ± 3.0	16.7 ± 0.6	2.5 ± 0.2
4893	15°52.3′N 82°09.1′E	28.7	33.60	15.5 ± 1.3	9.9 ± 0.8	1.6 ± 0.1
4895	15°07.9′N 83°05.6′E	29.6	33.85	11.5 ± 1.8	9.4 ± 0.3	1.2 ± 0.2
4897	14°57.0′N 81°37.0′E	29.2	33.61	10.1 ± 0.6	7.7 ± 0.3	1.3 ± 0.1
4898	15°26.5′N 81°06.0′E	28.5	33.83	12.5 ± 3.0	9.8 ± 0.4	1.3 ± 0.2
4900	15°04.5′N 80°18.7′E	29.5	33.80	11.6 ± 0.6	8.6 ± 0.4	1.3 ± 0.1
4901	14°31.2′N 80°18.0′E	29.4	33.80	14.7 ± 2.4	8.7 ± 0.7	1.7 ± 0.2
4906	12°8.1′N 81°28.0′E	29.6	33.94	11.2 ± 2.7	8.6 ± 0.4	1.3 ± 0.3
4908	13°30.0′N 83°10.0′E	29.2	33.16	11.2 ± 1.1	8.5 ± 0.3	1.3 ± 0.2
4910	14°49.0′N 83°44.0′E	28.5	33.29	14.8 ± 1.6	9.6 ± 0.3	1.6 ± 0.2
4911	15°29.0′N 83°31.0′E	29.2	33.13	12.4 ± 0.7	8.4 ± 0.4	1.5 ± 0.1
4912	17°19.0′N 83°39.0′E	29.7	33.14	12.8 ± 1.5	10.2 ± 0.5	1.3 ± 0.1
VISAKHA-PATNAM	17°72′N 83°48′E	—	—	37.3 ± 2.8	41.9 ± 2.8	0.9 ± 0.1
SK-63 (March–April 1991)						
H-2	20°49′N 88°12.2′E	27.65	31.143	24.5 ± 1.4	9.9 ± 0.4	2.5 ± 0.2
H-3	20°37.3′N 88°14.9′E	28.05	31.367	25.7 ± 1.2	9.8 ± 0.3	2.6 ± 0.1
H-4	20°28′N 88°18.1′E	27.89	31.421	18.5 ± 1.3	8.9 ± 0.3	2.1 ± 0.2
H-7	20°08.4′N 88°23.5′E	27.51	32.044	13.2 ± 0.9	6.6 ± 0.2	2.0 ± 0.2
H-13	17°59.8′N 88°59.9′E	28.22	32.213	12.5 ± 1.2	6.2 ± 0.2	2.0 ± 0.2

Table 1. (Continued)

Station	Location	Temp °C	Salinity	^{228}Ra* (dpm/100 kg)	^{226}Ra* (dpm/100 kg)	[228/226]*
SK-63 (March–April 1991) (Continued)						
G-1	19°50.8′N 86°26.2′E	27.98	32.518	17.1 ± 1.0	8.1 ± 0.3	2.1 ± 0.1
G-2	19°45.5′N 86°27′E	27.69	32.054	17.7 ± 1.0	9.6 ± 0.3	1.9 ± 0.1
G-5	19°33.1′N 86°36.9′E	27.73	31.655	18.5 ± 1.2	8.8 ± 0.3	2.1 ± 0.2
G-8	19°03.1′N 86°59.6′E	28.66	32.204	15.2 ± 0.8	7.9 ± 0.2	1.9 ± 0.1
G-10	18°N 87°47.3′E	28.20	32.913	14.4 ± 1.1	7.9 ± 0.3	1.8 ± 0.2
G-11	17°15.6′N 88°17.3E	28.43	32.08	13.7 ± 1.1	8.6 ± 0.3	1.6 ± 0.1
F-1	18°50.6′N 84°43.4′E	28.35	33.638	11.9 ± 0.8	7.6 ± 0.2	1.6 ± 0.1
F-2	18°41.1′N 84°51.7′E	28.44	32.736	12.5 ± 1.0	6.7 ± 0.4	1.9 ± 0.2
F-5	18°27.7′N 85°06.5′E	28.14	34.093	13.7 ± 0.9	6.8 ± 0.2	2.0 ± 0.2
F-7	18°13.1′N 85°18.7′E	28.71	32.493	13.7 ± 1.2	8.8 ± 0.3	1.6 ± 0.1
F-9	17°42.5′N 85°45.1′E	28.46	32.461	12.7 ± 0.8	7.1 ± 0.2	1.8 ± 0.1
F-11	16°27.1′N 86°56.9′E	28.68	32.139	14.5 ± 1.1	7.9 ± 0.3	1.8 ± 0.2
E-1	17°24.7′N 83°14.8′E	28.73	32.312	22.8 ± 1.0	11.2 ± 0.3	2.0 ± 0.1
E-2	17°17.6′N 83°19.9′E	28.75	32.213	16.1 ± 0.9	8.5 ± 0.3	1.9 ± 0.1
E-4	17°11′N 83°24.6′E	28.78	32.300	16.5 ± 1.0	8.6 ± 0.3	1.9 ± 0.1
E-6	17°02.6′N 83°31.5′E	29.07	32.664	18.3 ± 1.1	9.5 ± 0.3	1.9 ± 0.1
E-8	16°50.8′N 83°44.3′E	28.88	32.523	17.3 ± 1.0	9.1 ± 0.3	1.9 ± 0.1
E-13	14°47.9′N 85°12.6′E	29.07	32.275	19.2 ± 1.0	9.6 ± 0.2	2.0 ± 0.1
D-2	16°06.9′N 81°55.4′E	28.90	32.637	21.7 ± 0.9	11.7 ± 0.3	1.9 ± 0.1
D-7	15°31.7′N 82°12.5′E	29.02	33.179	19.4 ± 1.0	10.1 ± 0.3	1.9 ± 0.1
C-8	14°N 81°3.8′E	29.03	32.169	23.1 ± 0.8	11.5 ± 0.2	2.0 ± 0.1

Table 1. (Continued)

Station	Location	Temp °C	Salinity	^{228}Ra* (dpm/100 kg)	^{226}Ra* (dpm/100 kg)	[228/226]*
SK-63 (March–April 1991) (Continued)						
C-2	14°00.2′N 80°20.6′E	28.02	34.364	12.1 ± 0.6	9.2 ± 0.2	1.3 ± 0.1
C-12	14°N 83°1.6′E	29.78	33.447	16.0 ± 1.2	9.8 ± 0.3	1.6 ± 0.1
B-4	12°40.5′N 80°39.4′E	28.99	32.932	21.1 ± 1.0	10.2 ± 0.3	2.1 ± 0.1
B-10	12°30.4′N 81°59.5′E	29.33	32.969	16.6 ± 0.9	9.7 ± 0.3	1.7 ± 0.1
A-2	10°42.8′N 80°6.2′E	29.43	33.611	13.2 ± 0.9	6.0 ± 0.3	2.2 ± 0.2
A-5	10°47.9′N 80°20.8′E	29.88	32.885	12.2 ± 1.0	6.4 ± 0.3	1.9 ± 0.2
A-10	10°59.6′N 81°59.5′E	29.81	32.682	15.4 ± 1.2	8.2 ± 0.4	1.9 ± 0.2
SK-70 (December 1991)						
D-1	16°14.3′N 81°53.3′E	26.14	28.530	28.0 ± 1.0	8.3 ± 0.3	3.4 ± 0.2
D-2	16°07.0′N 81°54.9′E	26.04	30.536	17.4 ± 0.9	6.0 ± 0.3	2.9 ± 0.2
D-4	15°55.3′N 82°01.2′E	27.06	33.316	13.5 ± 0.8	6.3 ± 0.2	2.1 ± 0.2
D-6	15°42.3′N 82°05.4′E	26.97	33.281	10.7 ± 0.7	6.1 ± 0.2	1.8 ± 0.1
D-9	14°55.9′N 82°33.8′E	27.21	33.154	11.8 ± 1.1	6.0 ± 0.3	2.0 ± 0.2
C-3	14°N 80°25.7′E	26.55	28.939	27.2 ± 1.2	8.5 ± 0.3	3.2 ± 0.2
C-5	14°00.2′N 80°37.3′E	27.01	29.827	35.9 ± 1.1	14.3 ± 0.3	2.5 ± 0.1
C-9	13°59.9′N 89°19.7′E	27.3	33.686	12.1 ± 0.8	7.4 ± 0.4	1.6 ± 0.1
C-12	13°56.1′N 83°04.8′E	27.36	33.839	12.5 ± 0.5	8.7 ± 0.2	1.4 ± 0.1
B-1	12°42.5′N 80°18.9′E	26.64	28.536	33.8 ± 1.1	13.6 ± 0.4	2.5 ± 0.1
B-4	12°39.5′N 80°39.7′E	26.94	31.980	22.8 ± 0.8	11.3 ± 0.2	2.0 ± 0.1
A-1	10°40.4′N 80°01.5′E	26.94	27.190	42.1 ± 1.1	14.2 ± 0.3	3.0 ± 0.1
A-3	10°44.9′N 80°12.0′E	26.96	28.566	35.3 ± 1.0	14.0 ± 0.3	2.5 ± 0.1
A-12	10°57.2′N 84°02.0′E	28.18	33.543	15.1 ± 0.8	8.8 ± 0.2	1.7 ± 0.1

Table 1. (Continued)

Station	Location	Temp °C	Salinity	^{228}Ra* (dpm/100 kg)	^{226}Ra* (dpm/100 kg)	[228/226]*
SS-152 (February 1997)						
3829	8°31.0′N 86°2.0′E	28.27	33.813	9.3 ± 0.5	7.4 ± 0.2	1.3 ± 0.1
3831	11°27.3′N 79°58.2′E	27.87	33.003	17.3 ± 0.6	9.9 ± 0.3	1.7 ± 0.1
3833	11°29.5′N 79°54.8′E	27.28	32.912	21.0 ± 0.7	10.1 ± 0.3	2.1 ± 0.1
3838	14°46.0′N 80°21.0′E	26.47	33.725	12.6 ± 0.5	8.0 ± 0.2	1.6 ± 0.1
3844	12°31.0′N 84°30.0′E	27.30	33.592	12.5 ± 0.6	8.4 ± 0.2	1.5 ± 0.1
SS-172 (February 1999)						
4028	17°30.0′N 85°59.8′E	26.95	32.615	19.2 ± 0.9	10.2 ± 0.4	1.9 ± 0.1
4030	18°56.0′N 89°32.3′E	26.17	32.327	21.1 ± 0.7	10.5 ± 0.3	2.0 ± 0.1
4031	16°55.0′N 91°08.4′E	26.10	32.588	17.8 ± 0.6	8.8 ± 0.2	2.0 ± 0.1
4041	4°58.5′N 85°53.5′E	28.76	34.500	6.8 ± 0.5	8.7 ± 0.2	0.8 ± 0.1

*Propagated one sigma errors are quoted; all values are rounded off to the first decimal place.

features suggest that the surface waters of the Bay of Bengal are fairly turbulent for a large part of the year.

4. Results

The measured concentrations of ^{228}Ra and ^{226}Ra along with [228/226] in the surface waters of the western Bay of Bengal collected during the five cruises are given in Table 1. ^{228}Ra along with [228/226] are plotted in the Figures 1a, b and c representing G-200, SK-63 and SK-70, respectively. Data from SS-152 and SS-172 are shown in Figure 1b along with SK-63, as the sampling period is February–March for these three cruises (Table 1). Though samples were collected at least 10 km away from the coastline to avoid localized and fluctuating Ra sources, one still notices some high values especially for ^{228}Ra and [228/226] as evident from Figures 1a and c. It is possible that submarine groundwater discharge (Moore, 1996; Buddemier, 2000) may be contributing to the high Ra values especially in the region south of 12N (Fig. 1a and c). The range and mean concentrations of Ra isotopes and [228/226] are given in Table 2. A few high ^{228}Ra, ^{226}Ra and [228/226] values were reported close to Kalpakkam, the site of major nuclear complex (Iyengar *et al.,* 1989). These are very shallow waters too

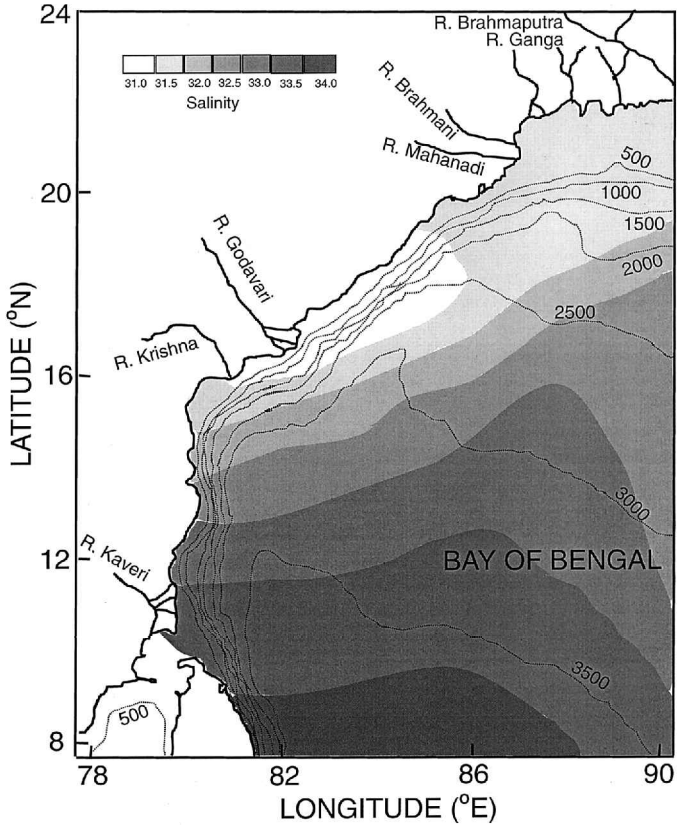

Figure 2. Map showing bathymetric contours (dotted lines) and mean annual surface salinity variations (grey shade contours) in the northern Bay of Bengal (Varkey *et al.,* 1996; Levitus, 2001).

close to the coast and their effect is not discernible beyond the sampling site. The ^{226}Ra concentration of the Indian Ocean surface waters by earlier workers (viz. 9–10 dpm/100 kg) fall in the overall range obtained in the present study (viz. 6–16.7 dpm/100 kg) except for one unusually high value of 41.9 dpm/100 kg near Visakhapatnam Port which receives a large amount of sewage from the city (Table 2). In general, during different seasons, ^{228}Ra and [228/226] decrease from coast to open, especially in the north-south direction. The ^{226}Ra concentrations do not show such a clear decrease, which is expected. A better way to understand these changes is through plots of isotope concentration and [228/226] as a function of salinity since the source regions are estuaries especially at low salinities (Carroll, 1990). Such plots are shown in Figures 3a, b and c. Regression analysis of the data (n = 71) yields the following equations:

Table 2. Range and mean of concentrations of ^{228}Ra and [228/226] activity ratio of the surface waters of the Bay of Bengal.

		^{228}Ra (dpm/100 kg)		^{226}Ra (dpm/100 kg)		[228/226]	
Cruise (period)	*n	Range	Mean	Range	Mean	Range	Mean
G-200 (Aug.–Sep. 1988)	15	10.1–41.9	17.7 ± 10.8	7.7–16.7	10.3 ± 2.6	1.2–2.6	1.6 ± 0.5
SK-63 (March 1991)	33	11.9–25.7	16.7 ± 3.9	6.0–11.7	8.7 ± 1.5	1.3–2.6	1.9 ± 0.2
SK-70 (Dec. 1991)	14	10.7–42.1	22.7 ± 10.8	6.0–14.3	9.5 ± 3.3	1.4–3.4	2.3 ± 0.6
SS-152 (Feb. 1997)	5	9.3–21.0	14.5 ± 4.6	7.4–10.1	8.8 ± 1.1	1.3–2.1	1.6 ± 0.2
SS-172 (Feb. 1999)	4	6.8–21.1	16.2 ± 6.4	8.7–10.5	9.5 ± 1.0	0.8–2.0	1.7 ± 0.6
All samples	71	6.8–42.1	17.8 ± 7.9	6.0–16.7	9.2 ± 2.2	0.8–3.4	1.9 ± 0.5

*n refers to number of samples.

$$^{228}\mathrm{Ra(dpm/100\,kg)} = (-4.396 \pm 0.004) \times \mathrm{salinity} + (160.2 \pm 0.2) \quad [r = -0.787, P < 0.005] \tag{1}$$

$$^{226}\mathrm{Ra(dpm/100\,kg)} = (-0.634 \pm 0.023) \times \mathrm{salinity} + (29.5 \pm 0.8) \quad [r = -0.461, P < 0.005] \tag{2}$$

$$[228/226] = (-0.262 \pm 0.009) \times \mathrm{salinity} + (10.34 \pm 0.29) \quad [r = -0.825, P < 0.005] \tag{3}$$

It is clearly seen that both ^{228}Ra, ^{226}Ra concentration and [228/228] decrease with increasing salinity. The best fit lines through the data (Fig. 3a, b and c) yield ^{228}Ra and ^{226}Ra concentrations of ~107 and 21.2 dpm/100 kg respectively and [228/226] = 6.9 at salinity = 13 where Ra isotope concentrations reach their maximum values. It is in this low to mid salinity region that Ra isotopes show high concentrations (Elsinger and Moore, 1983). The predicted and measured values in this estuarine region (Carroll, 1990; Somayajulu *et al.,* 2002) are in reasonable agreement. In the case of ^{226}Ra no significant variation in its concentration is noticed (Fig. 3b). It is reasonable to assume that ^{226}Ra is about uniformly distributed in the Bay of Bengal surface waters averaging 9.2 ± 2.2 dpm/100 kg (Table 2, Fig. 4) irrespective of seasons. This is expected in view of the turbulence of the Bay of Bengal surface waters due to monsoons and cyclones. The only calm period in the Bay of Bengal is mid-January to mid-March when the half-life of ^{226}Ra is long. Hence, significant variations could be expected only for short-lived nuclides, e.g. ^{228}Ra. Since the change in ^{226}Ra concentration is small, the [228/226] is expected to follow

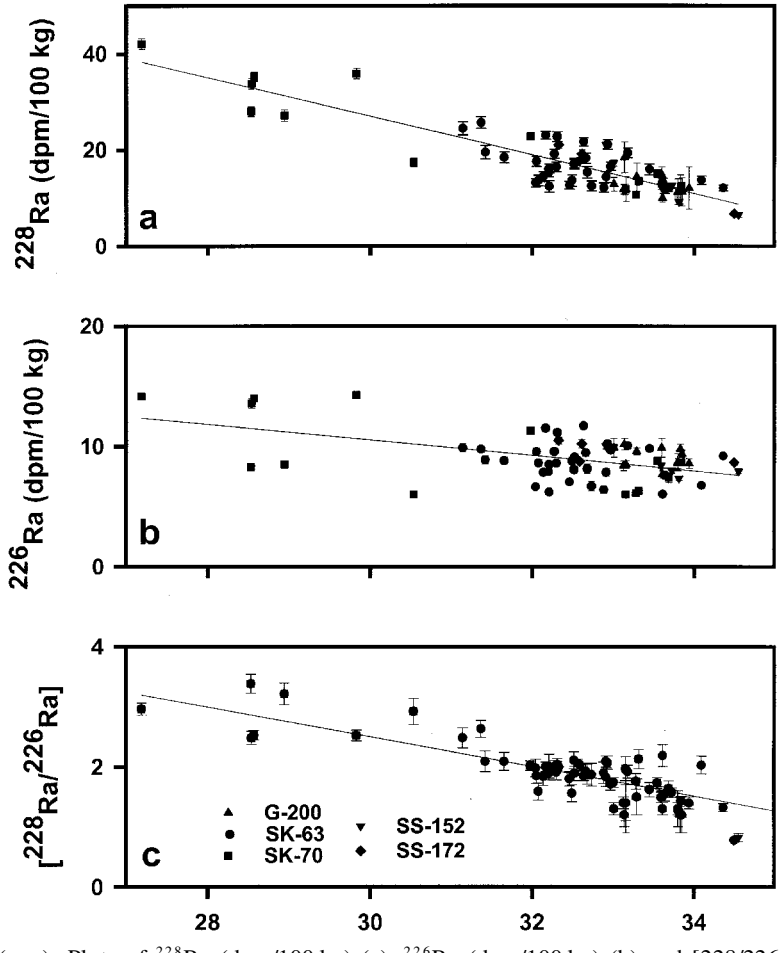

Figure 3(a–c). Plots of ^{228}Ra (dpm/100 kg) (a), ^{226}Ra (dpm/100 kg) (b) and [228/226] (c) as a function of salinity in the surface waters of the western Bay of Bengal. Notice the change of scale in *y*-axis for different plots. See text for discussion.

the distribution of ^{228}Ra, which is evident from Figure 3c. Even in estuaries (salinity = 2–20) where Ra isotopes are excessively released into the seawater, the [228/226] values do not exceed 3–5 (Elsinger and Moore, 1983; Somayajulu *et al.,* 2002).

5. Discussion

As seen in the previous section, the surface salinity in the Bay of Bengal shows a dominantly decreasing trend from north to south. The west to east trend is not as clear since the freshwater discharges from the Indian peninsular rivers is much less than that of the Ganga-Brahmaputra system. This kind of consistent trend across the bay (from north to

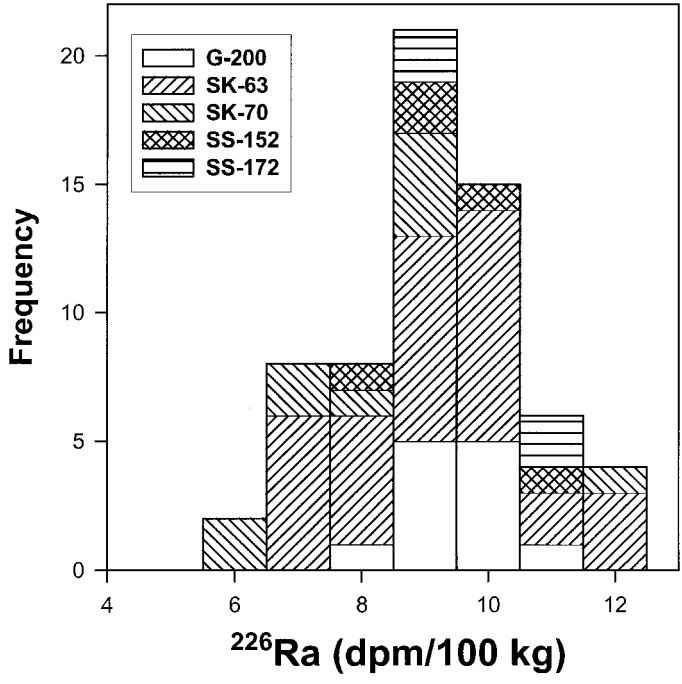

Figure 4. Frequency plot ^{226}Ra in the surface waters of the western Bay of Bengal. The peak concentrations lie between 8.5 and 9.5 dpm/100 kg.

south) is a result of the mixing of low salinity waters entering from the Ganga-Brahmaputra estuarine system with the high salinity waters in the south. As it is shown that Ra isotopes especially ^{228}Ra (and [228/226]) have a strong inverse correlation with salinity, one can use the Ra isotope distribution to evaluate time scales of mixing of surface waters.

a. One-dimensional model

^{228}Ra has been used as a tracer to estimate eddy diffusivity of coastal waters across the shelf. Several groups used the distribution of ^{228}Ra in continental shelf waters to determine horizontal mixing rates across the shelf (Kaufman *et al.,* 1973; Brewer and Spencer, 1975; Knauss *et al.,* 1978). The observed gradient in ^{228}Ra concentrations in surface water between coastline and central sites is supposed to reflect eddy diffusion of ^{228}Ra. In the simplest case, the ^{228}Ra distribution can be treated as a balance between eddy diffusion and radioactive decay of ^{228}Ra. At steady state,

$$K_h(d^2C/dx^2) - \lambda C = 0 \tag{4}$$

where C is the concentration of ^{228}Ra, λ the decay constant of ^{228}Ra (3.83×10^{-9} s^{-1}) and x is the distance offshore. With boundary conditions $C = C_0$ at $x = 0$ and $C = 0$ at $x = \infty$, the solution of (4) is

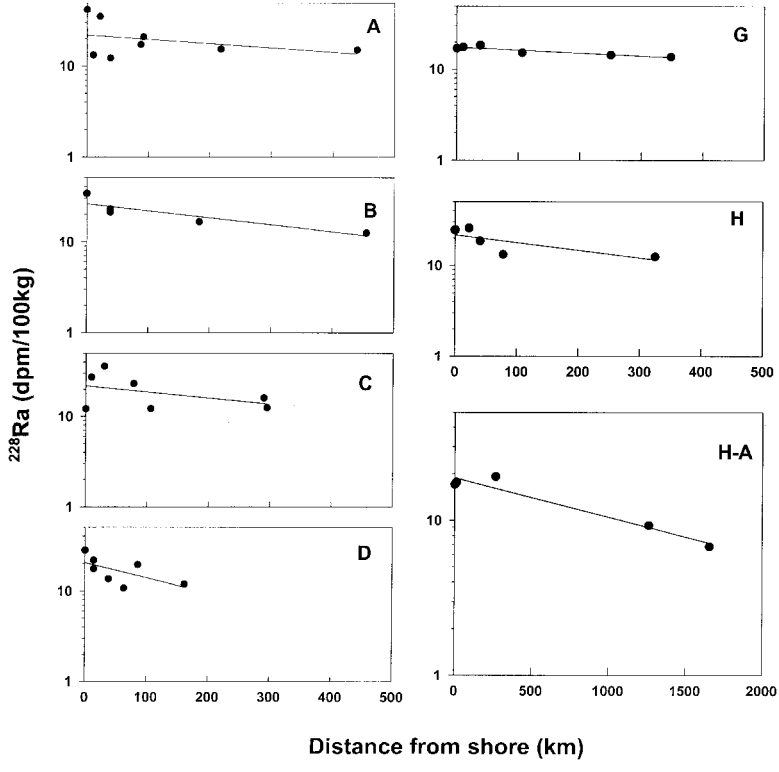

Figure 5. Plots showing ^{228}Ra versus distance from the coast along the six coast-to-open-ocean tracks denoted by letters A to H. H–A denotes north to south track comprising ^{228}Ra data from all available samples on this track. Data (especially in panels A, C, D) show considerable scatter, see text for discussion.

$$C = C_0 \exp(-x/x^*) \text{ where } x^* = \sqrt{(K_h/\lambda)} \tag{5}$$

$$K_h = [x/\ln (C_0/C)]^2\lambda \tag{6}$$

where x is the distance between the two points, x^* the scale length and K_h the effective horizontal eddy diffusivity.

It should be pointed out here that in this model, K_h is assumed more dominant than surface currents and vertical mixing. In other words, advection, both in horizontal and vertical directions, is neglected. It is also known that in the near-coastal regions there can be deepening of the mixed layer with distance from the coast which is also neglected in this model. The straight-line trajectories in the west-east direction from seven coastal locations have been taken and the plots of ^{228}Ra versus distance from the coast are shown in Figure 5. These are the trajectories along which physical oceanographic data were collected during SK-63 and SK-70 cruises (Shetye *et al.,* 1996). In the two recent cruises SS-152 and SS-172, some surface samples were collected from the study region and these, if falling in

Table 3. Effective eddy diffusivities using horizontal transects from the shore of the Bay of Bengal.

		Eddy diffusivity (10^6 cm^2 s^{-1})		
Direction	Leg	SK-63 March 1991	SK-70 Dec. 1991	Both data
W–E	A	17.2†	4.0	15.7
W–E	B	12.7	1.7	6.2
W–E	C	11.0	1.9	7.9
NW–SE	D	24.7	1.2	39.0
NW–SE	G	31.7	—	—
NNW–SSE	H	5.1	—	—
N–S		56	—	—

†This value is calculated combining the data from SS-152 and SS-172 cruises (Table 1).

these transects have also been used in the plots. The K_h values in the west-east direction, calculated using Eq. (6) are shown in Table 3, range from 5.1×10^6 to 2.5×10^7 cm^2 s^{-1} with a characteristic scale length of ~114–323 km. As seen from Table 3, the coast to open ocean cruise tracks are in the E–W, NW–SE direction. Available data for the N–S direction in the open ocean are used (Fig. 1b and Table 3) and the K_h is calculated to be 5.6×10^7 cm^2 s^{-1}. The overall range of K_h is between 5.1×10^6 and 56×10^6 cm^2 s^{-1}. These values match well with the empirical diffusion diagram shown by Okubo (1971) using dye-release experiment data in the upper mixed layer of the North Sea. Data from the two transects E and F (Fig. 1b) could not be used, as there is no decrease of ^{228}Ra with distance from the coast. The lack of ^{228}Ra decrease suggests the assumptions made in this model are perhaps not valid and that it cannot be applied on a large regional basis. Since there is a concentration gradient, despite scatter in the data along four transects (Fig. 5), it is used to get an idea of the ballpark K_h values. Moore (1987) tried to use a 1-D diffusion model in the south Atlantic Bight without success due to similar problems.

It is clear that with the fairly abundant data (Table 1), one needs a 2-D model with the inclusion of currents/advection in the horizontal directions. Earlier, an attempt in this direction was made by Somayajulu *et al.* (1996) where a 2-D diffusion model was used for similar data from the Arabian Sea. Huh and Ku (1998) also applied a similar model to the northeast Pacific region (off Baja, California).

b. Two-dimensional horizontal model

For surface measurements, a 2-D horizontal model is appropriate to deduce the mixing parameters since the mean annual salinity field of the western Bay of Bengal is a permanent feature (Fig. 2) and upwelling that brings low ^{228}Ra, ^{226}Ra waters to the surface (Sarin *et al.,* 1994) is not a dominant phenomenon in the Bay of Bengal compared to, for example, the Arabian Sea. It is therefore not unreasonable to assume

steady state. It is mentioned in the previous sections that the shoaling of D_{ml} does not arise once the near-coastal region is avoided. The two-dimensional steady-state mass balance equation for ^{228}Ra in the surface of the ocean, where this tracer behaves conservatively, can be expressed as

$$K_x \frac{\partial^2 C}{\partial x^2} + K_y \frac{\partial^2 C}{\partial y^2} - w_x \frac{\partial C}{\partial x} - w_y \frac{\partial C}{\partial y} - \lambda C = 0 \tag{7}$$

where C is the ^{228}Ra concentration (dpm/100 kg) in seawater; x and y refer the E–W (zonal) and S–N (meridional) directions (coordinates), respectively, positive eastward and northward and λC is the radioactive decay term. Besides radioactive decay, the ^{228}Ra budget is affected by turbulent transport into and out of a volume element, described in terms of horizontal eddy diffusivity (K_h) and horizontal advection (w) in both zonal and meridional directions. We proceed as follows: in the first instance, mixing is assumed to be diffusion dominated; i.e., advection terms are neglected. Later the diffusion terms are neglected making advection the dominant mixing process and finally both diffusion and advection are taken into account.

i. 2-D diffusion model. Neglecting advection terms, Eq. (7) reduces to

$$K_x \frac{\partial^2 C}{\partial x^2} + K_y \frac{\partial^2 C}{\partial y^2} - \lambda C = 0. \tag{8}$$

The source regions of Ra isotopes to the Bay of Bengal are distributed all along the coast with water and sediment discharging from several rivers, the most dominant contribution coming from the Ganga-Brahmaputra River system (Carroll *et al.,* 1993; Somayajulu *et al.,* 2002). The estuarine regions of rivers release large amounts of ^{228}Ra and ^{226}Ra and their concentrations vary as a function of the water discharge of the coastal rivers. This is especially true for the western Bay of Bengal where a large number of rivers discharge into it, of which six are major to large (Fig. 2). It, therefore, becomes difficult to fix boundary values for the ^{228}Ra (and ^{226}Ra) concentrations (like for example, those for the western Arabian Sea (Somayajulu *et al.,* 1996). To avoid this problem, the solution to Eq. (8) in the analytical form is assumed to be

$$C_{(x,y)} = C_0 e^{-Ax} \cdot e^{-By} \tag{9}$$

which can be rewritten as

$$\log C_{(x,y)} = \log C_0 - By - Ax. \tag{10}$$

By fitting the analytical form to the data, A, B and C_0 are estimated using least squares method (Bevington, 1969). This model is applied to the ^{228}Ra data from the western Bay of Bengal and the distribution of measured as well as the model-based ^{228}Ra concentration are shown in Figures 6a and b. Six data points with high values of ^{226}Ra (>14 dpm/100 kg) near the coast are removed (Fig. 1a and c). These high concentrations may be due to the

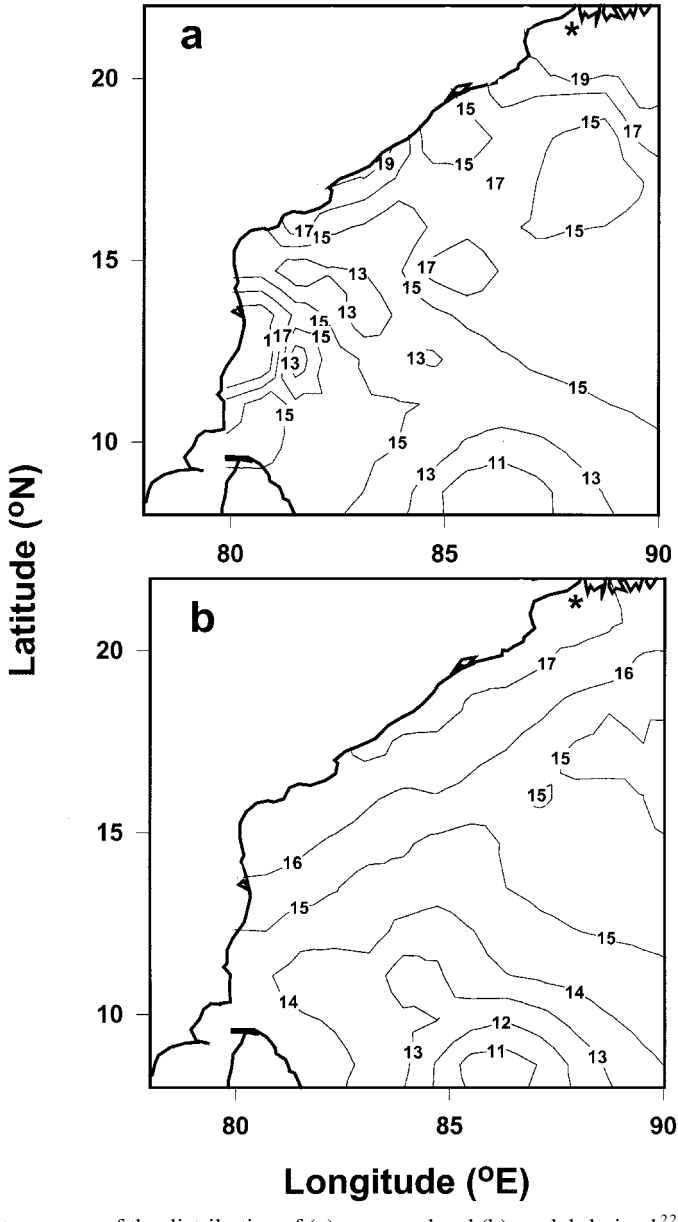

Figure 6. Contour maps of the distribution of (a) measured and (b) model-derived ^{228}Ra concentration (dpm/100 kg) in the surface waters of the western Bay of Bengal. Model reproducibility is good.

groundwater recharge into the Bay of Bengal during the lean-flow period (Moore, 1996; 1997). Distances in both x and y directions are calculated by taking 22N 88E as origin (indicated by asterisk in Fig. 1b) and the C_0 value obtained for ^{228}Ra is 18.5 dpm/100 kg which is close to the values measured in this region. Since the Ganga-Brahmaputra estuarine waters as well as those of the Hooghly River have the highest ^{228}Ra, ^{226}Ra and [228/226], the choice of the location as origin is reasonable. Except for the coastal high values, other features are reasonably well reproduced by the model (Fig. 6). The values obtained for A and B are 0.3067×10^{-6} and $-0.4234 \times 10^{-6}\,m^{-1}$, respectively. The estimated errors on these values are about 50%; not alarmingly high considering the uneven distribution of the sampling locations in the western Bay of Bengal. It should be mentioned here that the choice of origin has no effect on the model-derived data as well as on the deduced mixing parameters (K, w or both) and reproduces the contours of the measured ^{228}Ra data. Constants A and B are independent of the chosen origin. One can select origin anywhere and the C_0 concentrations as well as constants A and B are computed by the least square fit. In the case of ^{226}Ra, the model values are in a narrow range, 8.4–8.8 dpm/100 kg which are much smaller than the measured ones (Fig. 7a and b). This is probably not unexpected considering the small λ of ^{226}Ra. In order to set up two equations to determine K_x and K_y, it was considered ^{226}Ra to be more suitable than other conventional oceanographic parameters.

Substituting $C_{(x,y)}$ in Eq. (8), the estimated constants A and B can be related to eddy diffusivities as:

$$K_x A^2 + K_y B^2 = \lambda \tag{11}$$

By using the distribution of ^{228}Ra and ^{226}Ra concentrations in the Bay of Bengal the following two equations are obtained so that the two unknowns K_x and K_y can be determined.

$$K_x A_{228}^2 + K_y B_{228}^2 = \lambda_{228} \tag{12}$$

$$K_x A_{226}^2 + K_y B_{226}^2 = \lambda_{226} \tag{13}$$

where subscripts 228 and 226 correspond to the values derived from ^{228}Ra and ^{226}Ra data, respectively. A_{228}, B_{228}, A_{226} and B_{226} obtained for the western Bay of Bengal data are 0.3067×10^{-6}, -0.4234×10^{-6}, 0.7642×10^{-7} and $-0.1718 \times 10^{-7}\,m^{-1}$ respectively, λ_{228} is $3.83 \times 10^{-9}\,s^{-1}$ and λ_{226} is $1.3725 \times 10^{-11}\,s^{-1}$. By solving these two equations, K_x and K_y are obtained to be 1.3×10^7 and $2.1 \times 10^8\,cm^2\,s^{-1}$, respectively. Whereas K_x is about the same K_y is about an order of magnitude higher compared to their Arabian Sea counterparts (Somayajulu *et al.,* 1996). Eddy diffusivities in the tropical Pacific Ocean have recently been derived by Bauer *et al.* (2002) using the Lagrangian surface drifting buoy data obtained from EPOCS (Equatorial Pacific Ocean Climate Study) and TOGA (Tropical Ocean Global Atmosphere)

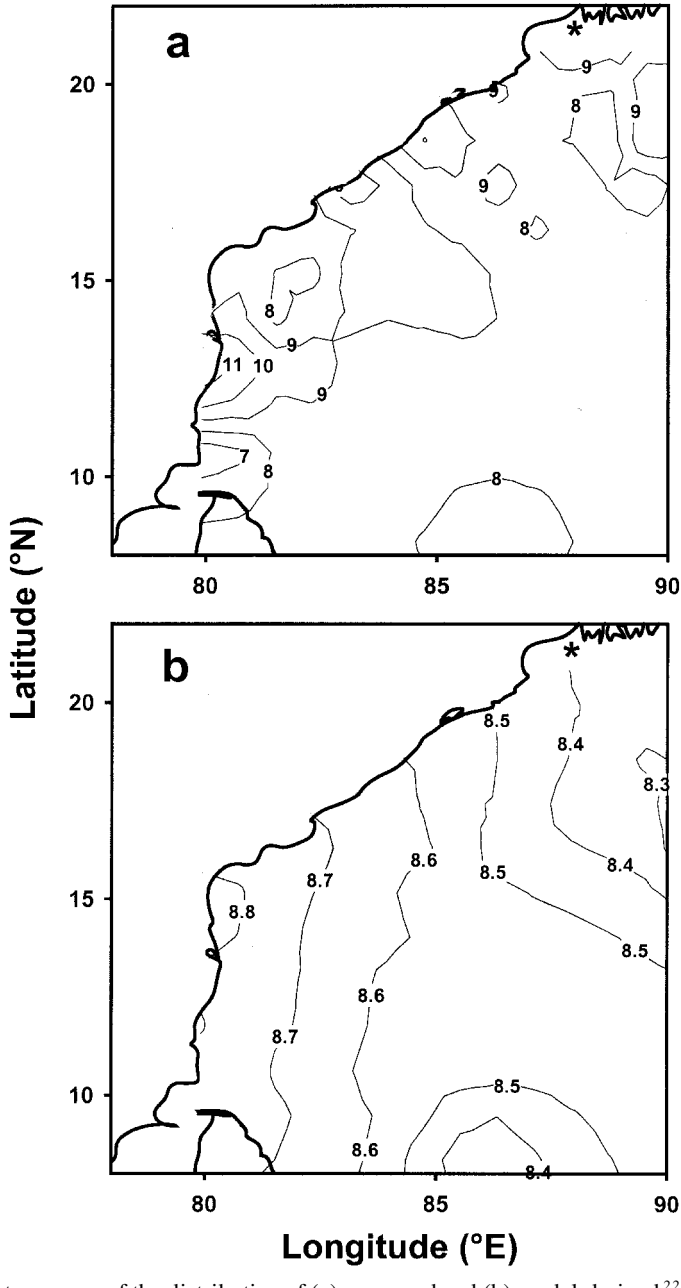

Figure 7. Contour maps of the distribution of (a) measured and (b) model-derived ^{226}Ra concentration (dpm/100 kg) in the surface waters of the western Bay of Bengal. Whereas measured values range from 8–12 dpm/100 kg, model contours range from 8–9 dpm/100 kg. See text for discussion.

studies. The zonal eddy diffusivities (K_x) ranged from 5×10^7 to 7.6×10^8 cm^2 s^{-1} higher than the meridional eddy diffusivities (K_y) which varied from 2×10^7 to 9×10^7 cm^2 s^{-1}. The K_x and K_y derived for the western Bay of Bengal are in the same general range, only the meridional mixing appears faster than the zonal when compared with the tropical Pacific Ocean.

ii. 2-D advection model. By neglecting the influence of diffusion and assuming the distribution of the Ra isotopes in the western Bay of Bengal is due to horizontal advection and radioactive decay only, one can obtain, by substituting $C_{(x,y)}$ in Eq. (4), the following relation:

$$w_x A + w_y B = \lambda. \tag{14}$$

As before, two equations for ^{228}Ra and ^{226}Ra are set up:

$$w_x A_{226} + w_y B_{226} = \lambda_{226} \tag{15}$$

$$w_x A_{228} + w_y B_{228} = \lambda_{228}. \tag{16}$$

Solving Eqs. (15) and (16), w_x and w_y are determined to be -0.2 and -1.1 cm s^{-1}. The negative sign indicates (in both w_x and w_y) that the effective advection is in the N–S and E–W directions, respectively. The distances in both x and y directions are computed by taking 22N 88E as origin. Like eddy diffusivity, the advection velocity is higher in meridional direction relative to zonal direction. Surficial currents (depth 5 m) in the Bay of Bengal mainly depend on wind intensities and are deduced to be in the region of 1–5 cm s^{-1} (McCreary *et al.,* 1996). Surface currents in the Bay derived from satellite tracked Lagrangian surface drifting buoy data by Shenoi *et al.* (1999) are $<$10 cm s^{-1}, about an order of magnitude faster than the ones deduced presently. Note that comparison is between advection measured for a short period and that averaged over the mean-life of ^{228}Ra, viz. $\sim$8 y (present study).

iii. 2-D advection-diffusion model. To see the effect of advection/current, advection terms are included in Eq. (11).

$$K_x A^2 + K_y B^2 + w_x A + w_y B = \lambda \tag{17}$$

$$K_x A^2 + K_y B^2 = \lambda - w_x A - w_y B$$

$$K_x = \frac{\lambda - w_x A - w_y B}{A^2} - \frac{K_y B^2}{A^2}$$

$$K_x = \frac{\lambda - w_x A - w_y B}{A^2}\left[1 - \frac{K_y B^2}{\lambda - w_x A - w_y B}\right].$$

Similarly,

$$K_y = \frac{\lambda - w_x A - w_y B}{B^2}\left[1 - \frac{K_x A^2}{\lambda - w_x A - w_y B}\right]$$

or

$$K_x = \frac{k_1}{A}\left[\frac{\lambda}{A} - w_x - \frac{w_y B}{A}\right] \tag{18}$$

$$K_y = \frac{k_2}{B}\left[\frac{\lambda}{B} - w_y - \frac{w_x A}{B}\right] \tag{19}$$

where $\lambda = 3.83 \times 10^{-9}\ s^{-1}$, $A = 0.3067 \times 10^{-6}\ m^{-1}$, $B = -0.4234 \times 10^{-6}\ m^{-1}$ (A and B obtained using ^{228}Ra data) and $k_1 + k_2 = 1$. Giving equal weightage to k_1 and k_2 (i.e. 0.5), one can vary w_x and w_y over a wide range of values to see the effect of w on K. The term that controls K is λ/A (also λ/B) which has the dimension of velocity, the values are $\lambda/A = 1.2\ cm\ s^{-1}$ and $\lambda/B = -0.90\ cm\ s^{-1}$. Only when $(w_x + w_y) < \lambda/A$ and $(w_x + w_y) < \lambda/B$ will the K_x and K_y reduce from $10^8\ cm^2\ s^{-1}$ to lower values. Variations of K_x and K_y are considered with varying w_x and w_y. Here directions too are important, two cases are considered.

i) Zonal advection velocity, w_x is west to east (i.e. positive value) and meridional velocity w_y is north to south (negative value). The variations of K_x and K_y are shown in Figures 8a and b, respectively. The eddy diffusivities decrease with increasing velocities, the decrease is slower in the zonal direction compared to meridional one (Fig. 8a).

ii) Both w_x and w_y are kept positive (i.e. in west to east and south to north direction, respectively). K_x (Fig. 8c) and K_y (Fig. 8d) steeply increase with increasing w values, w_y having more effect on both K_x and K_y compared to w_x. The above calculations can be made with changing w_x and by changing both. Overall the eddy diffusivities increase or decrease depending on the direction of advection. Meridional mixing appears somewhat faster than zonal.

6. Conclusions

To the ^{228}Ra and ^{226}Ra concentrations measured in the surface waters during five cruises to the western Bay of Bengal, a 2-D advection-diffusion model is applied to derive the surface mixing parameters. Eddy diffusivities (K_x and K_y) ranging from $\sim 10^7$ to $\sim 10^9\ cm^2\ s^{-1}$ and advection velocities ranging from $\sim 10^{-2}$ to $\sim 1\ cm\ s^{-1}$ are needed to maintain the Ra isotope distribution which translates into the observed mean annual salinity distribution in the western Bay of Bengal. One needs more measurements covering the entire Bay during southwest monsoon and non-monsoon

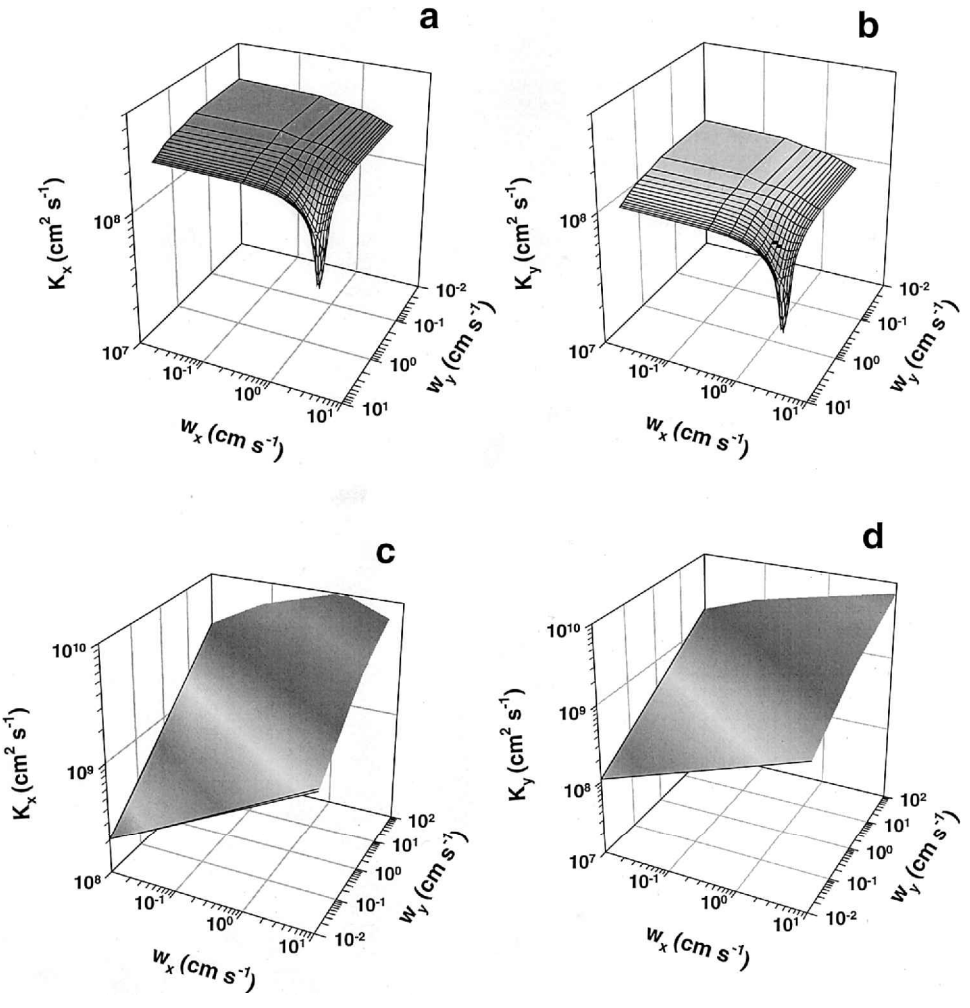

Figure 8. Plots of K versus w_x and w_y. In (a) and (b) K_x and K_y variations are shown, respectively, with increasing w_x (west to east) and w_y (north to south). With the increase in w_x and w_y, K decreases in both cases. K_x and K_y variations are shown with increasing w_x (west to east) and w_y (south to north) in (c) and (d), respectively. Notice the y-axis scales are reversed (compared to (a) and (b)) to show the abrupt increases in K_x and K_y. See text for discussion.

seasons to better understand the surface mixing processes and their temporal variations, if any.

Acknowledgments. We thank the officers and crew of the R/V *Gaveshani,* ORV *Sagar Kanya* and FORV *Sagar Sampada* for their assistance during sample collection. We also thank Mr. V. Ravindranathan, Director, CMLRE, Cochin and his staff for additional help concerning FORV *Sagar Sampada* cruises. Mr. J. P. Bhavsar provided help both in shipboard operations and in

manganese fiber processing. The authors thank Professor R. Ramesh and Prof. S. Krishnaswami for fruitful discussions. This study was in part supported by the Departments of Ocean Development and Space, Government of India. BLKS is thankful to CSIR and PRL/DOS for providing Emeritus Scientistship and Honorary Professorship, respectively, during the course of this study. We are thankful to the two reviewers for critical comments that improved the manuscript considerably.

REFERENCES

Bauer, S., M. S. Swenson and A. Griffa. 2002. Eddy-mean flow decomposition and eddy-diffusivity estimates in the tropical Pacific Ocean 2. Results. J. Geophys. Res. (In press).

Bevington, P. R. 1969. Data reduction and error analysis for the Physical Sciences, McGraw-Hill, 336 pp.

Brewer, P. G. and D. W. Spencer. 1975. Minor element models in coastal waters, *in* Marine Chemistry in Coastal Environment. ACS Symposium Ser., 18, T. M. Church, ed., American Chemical Society, Washington, DC, 80–96.

Broecker, W. S., J. Goddard and J. L. Sarmiento. 1976. The distribution of ^{226}Ra in the Atlantic Ocean. Earth Planet. Sci. Lett., *32,* 220–235.

Buddemier, R. W. (ed.) 2000. Groundwater discharge into the coastal zone. Proc. Intl. Symp., LOICZ-IGBP/R&S/96-8, LOICZ, Texal, The Netherlands, 179 pp.

Carroll, J. L. 1990. Processes which control the distribution of radium and uranium in the Ganges-Brahmaputra delta and their fluxes to the Bay of Bengal, Ph.D. Dissertation, Univ. South Carolina, Columbia SC, U.S.A., 118 pp.

Carroll, J. L., K. K. Falkner, E. T. Brown and W. S. Moore. 1993. The role of Ganges and Brahmaputra mixing zone in supplying barium and ^{226}Ra to the Bay of Bengal. Geochim. Cosmochim. Acta, *57,* 2981–2990.

Chung, Y. 1980. Ra-Ba-Si relations and a two-dimensional model for the World Ocean. Earth Planet. Sci. Lett., *49,* 309–318.

Elsinger, R. J. and W. S. Moore. 1983. ^{224}Ra, ^{228}Ra and ^{226}Ra in Winyah Bay and Delaware Bay. Earth Planet. Sci. Lett., *64,* 430–436.

Huh, C-A. and T-L. Ku. 1998. A 2-D section of ^{228}Ra and ^{226}Ra in the Northeast Pacific. Oceanol. Acta, *21,* 533–542.

Iyengar, M. A. R., V. Kannan and K. Narayana Rao. 1989. ^{228}Ra/^{226}Ra ratios in coastal waters of Kalpakkam. J. Environ. Radioactivity, *9,* 163–180.

Johns, B. 1981. Numerical simulation of storm surges in the Bay of Bengal, *in* Monsoon Dynamics, J. Lighthill and R. P. Pearce, eds., Cambridge University Press, Cambridge, 690–705.

Kaufman, A., R. Trier and W. S. Broecker. 1973. Distribution of ^{228}Ra in the world ocean. J. Geophys. Res., *78,* 8827–8848.

Knauss, K. G., T.-L. Ku and W. S. Moore. 1978. Radium and thorium isotopes in the surface waters of the east Pacific and coastal southern California. Earth Planet. Sci. Lett., *39,* 235–249.

Koczy, F. F. 1958. Natural radium as a tracer in the ocean. Proc. Second U.N. Int. Conf. Peaceful Uses of Atomic Energy, P/2370, Geneva, *18,* 351–357.

Ku, T.-L. and S. Luo. 1994. New appraisal of radium-226 as a large-scale oceanic tracer. J. Geophys. Res., *99,* 10255–10273.

La Fond, E. C. and K. G. La Fond. 1968. Studies of oceanic circulation in the Bay of Bengal. Proc. Symp. Indian Ocean, Bull. National Inst. Sci. India, *1,* 169–183.

Levitus, S. 2001. IRI/LDEO Climate Data Library, http://ingrid.ldgo.columbia.edu/SOURCES/.LEVITUS/.ANNUAL/.sal/

McCreary, J. P., W. Han, D. Shankar and S. R. Shetye. 1996. Dynamics of the East India Coastal Current, 2, Numerical solutions. J. Geophys. Res., *101,* 13993–14010.

Milliman, J. D. 1981. Transfer of river-borne particulate material to the ocean, *in* River Inputs to Ocean Systems, UNEP and UNESCO, Nairobi, Kenya, 116–131.

Milliman, J. D. and R. H. Meade. 1983. World-wide delivery of river sediment to the oceans. J. Geol., *91,* 1–29.

Moore, W. S. 1976. Sampling ^{228}Ra in the deep ocean. Deep-Sea Res., *23,* 647–651.

——— 1984. Ra isotope measurements using germanium detectors. Nucl. Instrum. Meth., *233,* 407–411.

——— 1987. ^{228}Ra in the south Atlantic Bight. J. Geophys. Res., *92,* 5177–5190.

——— 1996. Large groundwater inputs to coastal waters revealed by ^{226}Ra enrichments. Nature, *380,* 612–614.

——— 1997. High fluxes of radium and barium from the mouth of the Ganges-Brahmaputra River during low river discharge suggest a large groundwater source. Earth Planet. Sci. Lett., *150,* 141–150.

——— 1999. Application of ^{226}Ra, ^{228}Ra, ^{223}Ra and ^{224}Ra in coastal waters to assessing coastal mixing rates and groundwater discharge to oceans, *in* Isotopes in the Solar System, J. N. Goswami and S. Krishnaswami, eds., Indian Academy of Sciences, Bangalore, 109–116.

Nozaki, Y., V. Kasemsupaya and H. Tsubota. 1990. The distribution of ^{228}Ra and ^{226}Ra in the surface waters of the North Pacific. Geochem. J., *24,* 1–6.

Okubo, A. 1971. Oceanic diffusion diagrams. Deep-Sea Res., *18,* 789–802.

Pant, G. B. and K. Rupa Kumar. 1997. Climates of South Asia, John Wiley and Sons, NY, 320 pp.

Potemra, J. T., M. E. Luther and J. J. O'Brien. 1991. The seasonal circulation of the upper ocean in the Bay of Bengal. J. Geophys. Res., *96,* 12667–12683.

Rutgers Van der Loeff, M. M., R. M. Key, J. Scholten, D. Bauch and A. Michel. 1995. ^{228}Ra as a tracer for shelf water in the Arctic Ocean. Deep Sea Res. II, *42,* 1533–1553.

Sarin, M. M., R. Rengarajan and B. L. K. Somayajulu. 1994. Natural radionuclides in the Arabian Sea and Bay of Bengal—Distribution and evaluation of particle scavenging processes. Proc. Ind. Acad. Sci., *103,* 211–235.

Sarmiento, J. L., C. G. H. Rooth and W. S. Broecker. 1982. Radium-228 as a tracer of basin-wide processes in the abyssal ocean. J. Geophys. Res., *87,* 9694–9698.

Schmidt, S. and J.-L. Reyss. 1996. Radium as an internal tracer of Mediterranean outflow water. J. Geophys. Res., *101,* 3589–3596.

Shenoi, S. C., P. K. Saji and A. M. Almeida. 1999. Near-surface circulation and kinetic energy in the tropical Indian Ocean derived from Lagrangian drifters. J. Mar. Res., *57,* 885–907.

Shetye, S. R. 1993. The movement and implications of the Ganges-Brahmaputra run off on entering the Bay of Bengal. Curr. Sci., *64,* 32–38.

——— 1999. Dynamics of circulation of the waters around India, *in* Ocean Science: Trends and Future Directions, B. L. K. Somayajulu, ed., Indian National Science Academy, New Delhi, 1–21.

Shetye, S. R., A. D. Gouveia, D. Shankar, S. S. C. Shenoi, P. N. Vinayachandran, D. Sundar, G. S. Michael and G. Nampoothiri. 1996. Hydrography and circulation in the western Bay of Bengal during the northeast monsoon. J. Geophys. Res., *101,* 1401–14026.

Somayajulu, B. L. K., R. Bhushan, A. Sarkar, G. S. Burr and A. J. T. Jull. 1999. Sediment deposition rates on the continental margins of the eastern Arabian Sea using ^{210}Pb, ^{137}Cs and ^{14}C. Sci. Total Environ., *237/238,* 429–439.

Somayajulu, B. L. K., R. Rengarajan and R. A. Jani. 2002. Chemical and radiochemical studies in the Hooghly estuary, India, Mar. Chem. (in press).

Somayajulu, B. L. K., M. M. Sarin and R. Ramesh. 1996. Denitrification in the eastern Arabian Sea: Evaluation of the role of continental margins using Ra isotopes. Deep-Sea Res. II, *43,* 111–117.

Torgersen, T., K. K. Turekian, V. C. Turekian, N. Tanaka, E. DeAngelo and J. O'Donnell. 1996.

^{224}Ra distribution in surface and deep water of Long Island Sound: Sources and horizontal transport rates. Cont. Shelf Res., *16,* 1545–1559.

Unesco. 1971. Discharge of selected rivers of the world. Vol II and III, Paris.

Vinayachandran, P. N. 1995. The Bay of Bengal circulation in an ocean general circulation model, Ph.D. dissertation, Indian Inst. Sci., Bangalore. 167 pp.

Varkey, M. J., V. S. N. Murty and A. Suryanarayana. 1996. Physical oceanography of the Bay of Bengal and the Andaman Sea. Oceanog. Mar. Biol. Ann. Rev., *34,* 1–70.

Wyrtki, K. 1971. Oceanographic Atlas of the International Indian Ocean Expedition, National Science Foundation, Washington DC, 531 pp.

Received: *24 May, 2001;* revised: *13 November, 2001.*